# MATHEMATICAL MODEL OF THYRISTOR INVERTER INCLUDING A SERIES-PARALLEL RESONANT CIRCUIT

**M. Luft, E. Szychta**

*Faculty of Transport, Technical University of Radom, Poland*
*ul. Malczewskiego 29, 26-600 Radom, tel.: +48 48 361 70 10,*
*mail: m.luft@pr.radom.pl, e.szychta@pr.radom.pl*

**Summary** The article presents a mathematical model of thyristor inverter including a series-parallel resonant circuit with the aid of state variable method. Maple procedures are used to compute current and voltage waveforms in the inverter.

## 1. INTRODUCTION

Resonant thyristor inverters are applied in induction heating, welding, dielectric heating, and other areas where heating processes are utilised which occur effectively in broad frequency ranges. Design of the inverters includes a resonant circuit that overloads at the inverter's switching frequency [1, 2]. Voltage at load of resonant inverters is sinusoidal in nature where the inverter's operating frequency ranges from several hundred to a dozen thousand Hertz.

This article will present a mathematical model of the inverter's resonant circuit with the aid of operator state variable method by means of Maple software procedures.

## 2. DESIGN OF THE INVERTER

The main circuit of the inverter is show in Figure 1 [3, 4]. Inductance $L$ and resistance $R$ represent loads of the inverter. Capacitance C is a parallel capacitor to compensate reactive power. Capacitance $C_s$ constitutes a series capacitor that participates in oscillations of supply current $i_d$. The presence of $L_d$ affects the current nature of source supplying non-continuous current $i_d$. The choke $L_d$ also helps to restrict $di_d/dt$ of supply current conducted by thyristors and to reduce dynamic loses across thyristors.

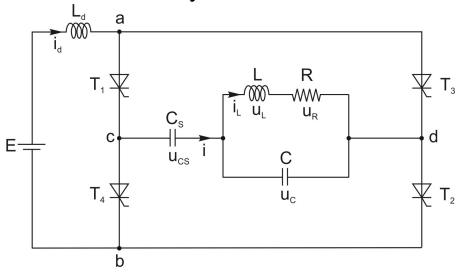


*Fig.1. The main circuit of the resonant inverter*

The authors assume that the inverter operates in the range of natural commutation [2]. Thyristors $T1$, $T2$ and $T3$, $T4$ are alternately switched on at frequency $f$ in time intervals $T/2$. The conductance angle of a thyristor pair is $\lambda$ ($\lambda < \pi$). (Fig.2).

## 3. MATHEMATICAL ANALYSIS OF THE INVERTER'S OPERATION

Mathematical analysis of electromagnetic phenomena in the inverter involves 4 magnitudes which are functions of time $t$: currents $i_L = i_L(t)$, $i_d = i_d(t)$ and voltages $u_C = u_C(t)$, $u_{CS} = u_{CS}(t)$ (Fig.1). Parameters of elements used in the converter's analysis conform with parameters of simulation model's elements as stated in Table 1.

*Table 1. Parameters of the inverter's elements*

| Parameter | $L$ | $R$ | $C$ | $E$ |
|---|---|---|---|---|
| Unit | [mH] | [Ω] | [μF] | [V] |
| | 0.139 | 0.25 | 218 | 540 |
| Parameter | $C_S$ | $L_d$ | $f$ | |
| Unit | [μF] | [mH] | [Hz] | |
| | 153 | 0.209 | 1000 | |

Four time intervals are distinguished in the inverter's operation cycle [4]. The mathematical analysis of currents and voltages of the inverter's resonant circuit is presented on the basis of the operator method [5]. The method implies that end conditions of each interval become initial conditions of the subsequent interval. Mathematical description of the inverter's operation in each of the intervals under analysis comprises systems of linear 1-st degree differential equations including the four magnitudes specified before, designated as state variables $x_i(t)$ at $i = 1 \div 4$.

$$i_L(t) = x_1(t),\ i_d(t) = x_2(t),\ u_C(t) = x_3(t),$$
$$u_{CS}(t) = x_4(t), \qquad (1)$$

The system of four differential equations that describe operation of the inverter in the $k^{th}$ time interval can be presented as a matrix:

$$\frac{d}{dt}\boldsymbol{X}k(t) = \boldsymbol{A}k \cdot \boldsymbol{X}k(t) + \boldsymbol{B} \cdot \boldsymbol{U}(t) \qquad (2)$$

where:

$$\boldsymbol{X}k(t)=\begin{bmatrix} xk_1(t) \\ xk_2(t) \\ xk_3(t) \\ xk_4(t) \end{bmatrix}=\begin{bmatrix} i_L^{(k)}(t) \\ i_d^{(k)}(t) \\ u_C^{(k)}(t) \\ u_{CS}^{(k)}(t) \end{bmatrix} \tag{3}$$

- state vector of the system in k[th] time interval ($k$=1,…,4),
where: $xk_i(t)$ - state variables in the system,
$\mathbf{A}k$ - system matrix for $k^{\text{th}}$ time interval,
$\boldsymbol{B}$ - control matrix,
$\boldsymbol{U}(t) = \mathbf{1}(t)$ – input function.

After Laplace transformation of (2), the transform $\boldsymbol{X}k(s)=\mathcal{L}[\boldsymbol{X}k(t)]$ of the (3) results:

$$\boldsymbol{X}k(s)=\boldsymbol{\Phi}k^{-1}\cdot\left\{\boldsymbol{X}k(0)+\boldsymbol{B}\cdot\frac{1}{s}\right\} \tag{4}$$

where: $\boldsymbol{\Phi}k=[s\boldsymbol{I}-\boldsymbol{A}k]$ - matrix inverse to $\boldsymbol{\Phi}k$ ,
$\boldsymbol{X}k(0)$ – initial conditions vector for $k^{\text{th}}$ time interval (values of variables $xk_i(0)$ at the start of $k^{\text{th}}$ interval).
Determinant of $\boldsymbol{\Phi}k$ is a characteristic polynomial $Mk(s)=\det\boldsymbol{\Phi}k$ of the transform (4). Roots of $Mk(s)$ have essential impact on the circuit's dynamics. The solution of (2) – the state vector $\boldsymbol{X}k(t)=\mathcal{L}^{-1}[\boldsymbol{X}k(s)]$ is the original transform (4).

Table 2 summarises factors in the differential equations that describe the inverter's dynamics in four consecutive time intervals. They depend on parameters of the circuit under analysis, presented in Table 1.

*Table 2. Factors in the differential equations that describe the inverter's operation in four time intervals*

| | | |
|---|---|---|
| $a=\frac{R}{L}$ | $b=\frac{1}{R}$ | $c=\frac{1}{L_d}$ |
| $g=\frac{E}{L_d}$ | $h=\frac{1}{C}$ | $k=\frac{1}{C_s}$ |

In the analysis of the inverter's operation, values of components of the initial condition vector $\boldsymbol{X}1(0)$ for the first time interval are determined on the basis of waveforms obtained in simulation testing of the inverter with the aid of Simplorer software [4]. Final conditions of each interval become initial conditions of the subsequent interval.

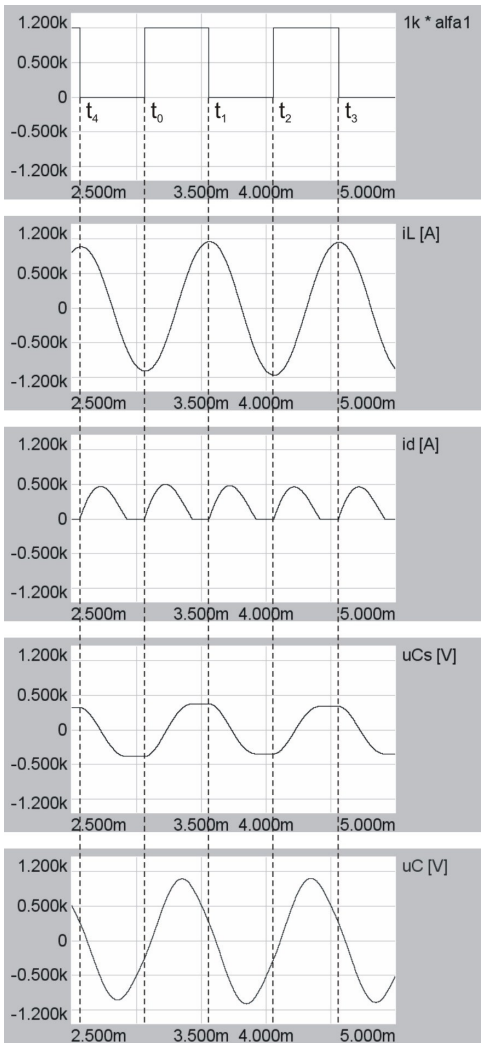


*Fig.2. Current and voltage waveforms in the inverter obtained from simulation; operating frequency f=1000Hz, output power P0=112kW*

Values of { $A_i^{(k)}$, $B_i^{(k)}$, $C_i^{(k)}$, $D_i^{(k)}$, $E_i^{(k)}$ } in the state variable expressions $xk_i(t)$ of the state vector $\boldsymbol{X}k(t)$ for k[th] time interval were determined with the help of Maple software.

**Interval 1**

In the first time interval: $t\in\langle t_0,t_1\rangle$ (Fig.2) $T1$ and $T2$ conduct. The resonant circuit for the first interval is shown in figure 3.

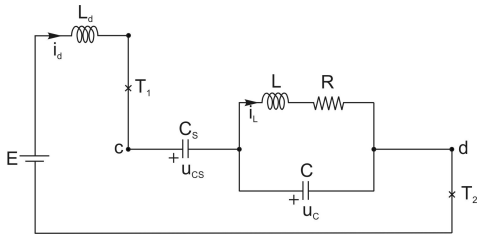


*Fig.3. Resonant circuit in the first time interval* $t\in\langle t_0,t_1\rangle$

The circuit in Figure3 is described in the differential equation (2) at $k$=1,

where:

$$\boldsymbol{X}1(t)=\begin{bmatrix} x1_1(t)\\ x1_2(t)\\ x1_3(t)\\ x1_4(t)\end{bmatrix},\ \boldsymbol{A}1=\begin{bmatrix} -a & 0 & b & 0\\ 0 & 0 & -c & -c\\ -h & h & 0 & 0\\ 0 & k & 0 & 0\end{bmatrix},\ \boldsymbol{B}1=\begin{bmatrix} 0\\ g\\ 0\\ 0\end{bmatrix} \tag{5}$$

Transform of the solution to $\mathbf{X}1(t)$ becomes (4) for $k$=1.

In the event, the characteristic polynomial $M1(s)$ becomes:

$$M1(s)=s^4+as^3+(hc+kc+hb)s^2+ac(h+k)s+hkbc \tag{6}$$

Taking into account values of {$a$, $b$, c, $h$, $k$} in Table 2, $M1(s)$ (6) becomes:

$$M1(s)=\left((s+m)^2+n^2\right)\left((s+p)^2+q^2\right) \tag{7}$$

where: $m=616.260$, $n=3762.815$, $p=283.020$, $q=8420.534$. Values of (10) roots were calculated using relevant procedures of Maple 10.

The vector of initial conditions $\boldsymbol{X}1(0)$ at $k$=1 is:

$$\boldsymbol{X}1(0)=\begin{bmatrix} x1_1(0)\\ x1_2(0)\\ x1_3(0)\\ x1_4(0)\end{bmatrix}=\begin{bmatrix} -883\\ 0\\ -267\\ -320\end{bmatrix} \tag{8}$$

Taking into account the initial conditions (8), the transform of $\boldsymbol{X}1(s)$ in the first time interval is:

$$\boldsymbol{X}1(s)=\begin{bmatrix} x1_1(s)\\ x1_2(s)\\ x1_3(s)\\ x1_4(s)\end{bmatrix}=\frac{1}{M_1(s)}\begin{bmatrix} L1_1(s)\\ L1_2(s)\\ L1_3(s)\\ \dfrac{L1_4(s)}{s}\end{bmatrix} \tag{9}$$

where:

$$L1_1(s)=-883s^3-267bs^2-883(hc+kc)s+$$
$$+320bhc+bhg-267bkc$$
$$L1_2(s)=(587c+g)s^2+(-883hc+587ca+ag)s+$$
$$+hbg+320hcb$$
$$L1_3(s)=-267s^3+(883h-267a)s^2+$$
$$+(hg-267kc+320hc)s+883khc$$
$$++ahg-267akc+320hca$$
$$L1_4(s)=-320s^4-320as^3+$$
$$+(kg-320hc-320hb+267kc)s^2+$$
$$+(-883khc+kag+267kca-320ahc)s+khbg$$

By determining originals of $x1_i(s)$ in the vector (9), system state variables $x1_1(t)\div x1_4(t)$ are expressed for the time interval $t\in\langle t_0,t_1\rangle$, ($t_0=3.067\cdot10^{-3}s$, $t_1=3.431\cdot10^{-3}s$). The initial time $t_{p1}=0$, duration of the first time interval $t_{k1}=t_1-t_0=0.364\cdot10^{-3}$ s are assumed. Waveforms of $x1_1(t)\div x1_4(t)$ in the first time interval $t\in\langle t_0,t_1\rangle$ are presented in Figures 4, 5, 6, 7.

$$x1_1(t)=i_L^{(1)}(t)=e^{(-mt)}\left(A_1^{(1)}\cos(nt)+B_1^{(1)}\sin(nt)\right)+$$
$$+e^{(-pt)}\left(C_1^{(1)}\cos(qt)+D_1^{(1)}\sin(qt)\right) \tag{10}$$

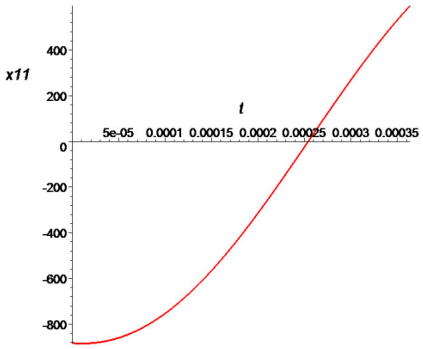


*Fig. 4. Interval 1 – the waveform of variable $x1_1(t)$ - current $i_L^{(1)}(t)$ at $t\in\langle t_0,t_1\rangle$*

$$x1_2(t)=i_d^{(1)}(t)=e^{(-mt)}\left(A_2^{(1)}\cos(nt)+B_2^{(1)}\sin(nt)\right)+$$
$$+e^{(-pt)}\left(C_2^{(1)}\cos(qt)+D_2^{(1)}\sin(qt)\right) \tag{11}$$

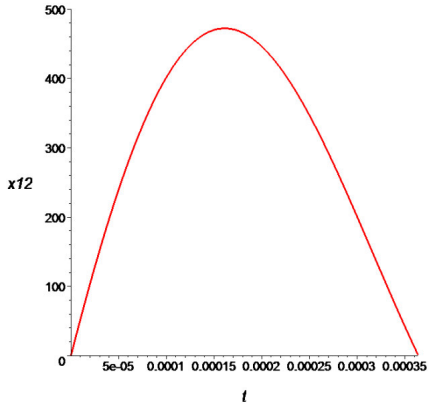


*Fig. 5. Interval 1 – the waveform of variable $x1_2(t)$ - current $i_d^{(1)}(t)$ at $t\in\langle t_0,t_1\rangle$*

$$x1_3(t)=u_C^{(1)}(t)=e^{(-mt)}\left(A_3^{(1)}\cos(nt)+B_3^{(1)}\sin(nt)\right)+$$
$$+e^{(-pt)}\left(C_3^{(1)}\cos(qt)+D_3^{(1)}\sin(qt)\right) \tag{12}$$

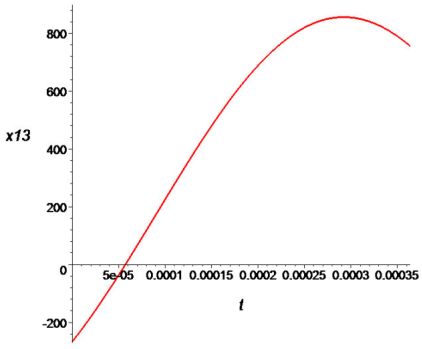


*Fig. 6. Interval 1 – the waveform of variable* $x1_3(t)$ *- voltage* $u_C^{(1)}(t)$ *at* $t \in \langle t_0, t_1 \rangle$

$$x1_4(t) = u_{CS}^{(1)}(t) = e^{(-mt)}\left(A_4^{(1)}\cos(nt) + B_4^{(1)}\sin(nt)\right) + \\ + e^{(-pt)}\left(C_4^{(1)}\cos(qt) + D_4^{(1)}\sin(qt)\right) + E_4^{(1)} \tag{13}$$

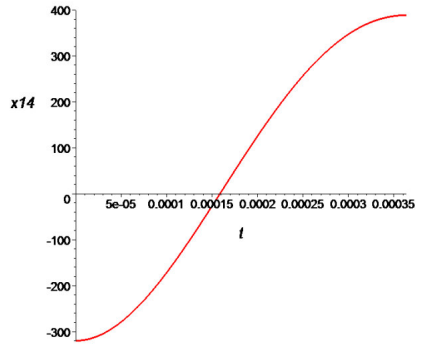


*Fig. 7. Interval 1 – the waveform of variable* $x1_4(t)$ *- voltage* $u_{CS}^{(1)}(t)$ *at* $t \in \langle t_0, t_1 \rangle$

End values $x1_i(t_{k1} = 0.364 \cdot 10^{-3})$ of $\mathbf{X}1(t)$ variables for the first interval become initial values of these variables in the second time interval:

$$\boldsymbol{X}1(t_k) = \begin{bmatrix} x1_1(t_k) \\ x1_2(t_k) \\ x1_3(t_k) \\ x1_4(t_k) \end{bmatrix} = \begin{bmatrix} 595 \\ 0.5 \\ 755 \\ 389 \end{bmatrix} = \boldsymbol{X}2(0) \tag{14}$$

**Interval 2**

The second time interval $t \in \langle t_1, t_2 \rangle$ (Fig.2) starts when $T1$, $T2$ are off and continues until $T3$, $T4$ are on. The resonant circuit switched off the supply voltage is illustrated in Figure 8. In the second time interval, supply current $i_d(t_2) = 0$ (Fig. 2).

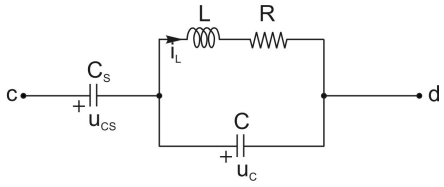


*Fig.8. Resonant circuit in the second time interval* $t \in \langle t_1, t_2 \rangle$

The circuit in Fig.8 is described in the system of differential equations (2) at $k$=2, where:

$$\boldsymbol{X}2(t) = \begin{bmatrix} x2_1(t) \\ x2_2(t) \\ x2_3(t) \\ x2_4(t) \end{bmatrix}, \boldsymbol{A}2 = \begin{bmatrix} -a & 0 & b & 0 \\ 0 & 0 & 0 & 0 \\ -h & 0 & 0 & 0 \\ 0 & 0 & 0 & 0 \end{bmatrix}, \boldsymbol{B}2 = \begin{bmatrix} 0 \\ 0 \\ 0 \\ 0 \end{bmatrix}$$

(15)

Transform of the solution to (16) has the form of (4) at $k$=2.

Characteristic polynomial $M2(s)$:

$$M2(s) = s^2\left(s^2 + as + hb\right) \tag{16}$$

Taking into account roots of (16), the characteristic polynomial $M2(s)$ can be presented:

$$M2(s) = s^2\left((s+g)^2 + r^2\right) \tag{17}$$

where: $g = 899.280$, $r = 5673.836$.

Taking into account the values of initial conditions vector (14) for $k$=2, transform of $\mathbf{X}2(s)$ in the second time interval results:

$$\boldsymbol{X}2(s) = \begin{bmatrix} x2_1(s) \\ x2_2(s) \\ x2_3(s) \\ x2_4(s) \end{bmatrix} = \begin{bmatrix} \dfrac{595s + 755b}{(s+g)^2 + r^2} \\ \dfrac{0{,}5}{s} \\ \dfrac{755s + 595h + 755a}{(s+g)^2 + r^2} \\ \dfrac{389}{s} \end{bmatrix} \tag{18}$$

By determining the originals of transforms $x2_i(t) = \mathcal{L}^{-1}\left[x2_i(s)\right]$ $(i = 1 \div 4)$ of (18), the system's state variables $x2_1(t) \div x2_4(t)$ are expressed for the time interval $t \in \langle t_1, t_2 \rangle$ ($t_1 = 3.431 \cdot 10^{-3}$ s, $t_2 = 3.559 \cdot 10^{-3}$ s). The waveforms of variables $x2_1(t) \div x2_4(t)$ in the second time interval $t \in \langle t_1, t_2 \rangle$ are presented in Figures 9, 10, 11, 12.

$$x2_1(t) = i_L^{(2)}(t) = e^{(-gt)}\left(A_1^{(2)}\cos(rt) + B_1^{(2)}\sin(rt)\right) \tag{19}$$

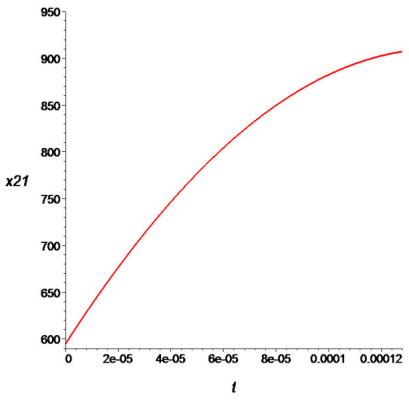


*Fig. 9. Interval 2 – the waveform of variable* $x2_1(t)$ *- current* $i_L^{(2)}(t)$ *at* $t \in \langle t_1, t_2 \rangle$

$$x2_2(t) = i_d^{(2)}(t) = 0.5 \tag{20}$$

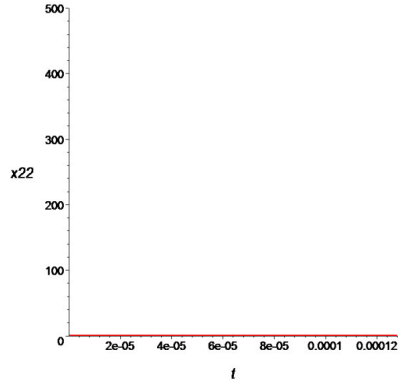


*Fig. 10. Interval 2 – the waveform of variable* $x2_2(t)$ *- current* $i_d^{(2)}(t)$ *at* $t \in \langle t_1, t_2 \rangle$

$$x2_3(t) = u_C^{(2)}(t) = e^{(-gt)}\left(A_3^{(2)}\cos(rt) + B_3^{(2)}\sin(rt)\right) \tag{21}$$

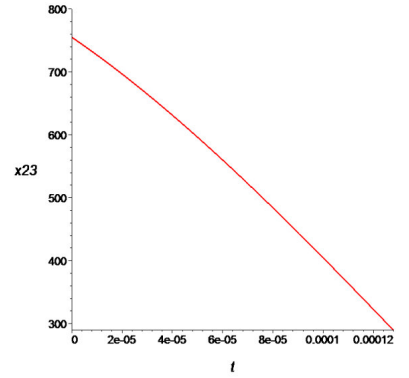


*Fig. 11. Interval 2 – the waveform of variable* $x2_3(t)$ *- voltage* $u_C^{(2)}(t)$ *at* $t \in \langle t_1, t_2 \rangle$

$$x2_4(t) = u_{CS}^{(2)}(t) = 389 \tag{22}$$

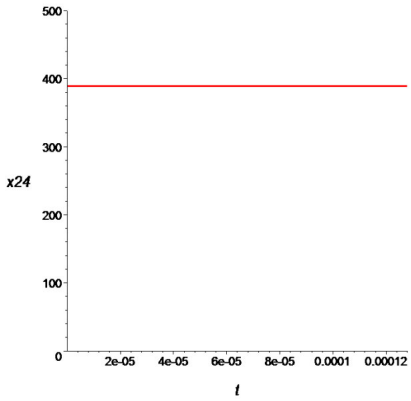


*Fig. 12. Interval 2 – the waveform of variable* $x2_4(t)$ *- voltage* $u_{CS}^{(2)}(t)$ *at* $t \in \langle t_1, t_2 \rangle$

Like in the previous time interval, the end values $x2_i(t_{k2} = 0.128 \cdot 10^{-3})$ of $\mathbf{X}2(t)$ variables for the second interval become the initial values of the same variables in the third time interval.

In the third time interval $t \in \langle t_2, t_3 \rangle$ (Fig.2), *T*3 and *T*4 are on. The resonant circuit for the third interval is shown in Figure 13. In this case, time waveforms are presented like in the first interval, with the initial conditions of the third interval assume end values of variables in the second operating interval of the inverter.

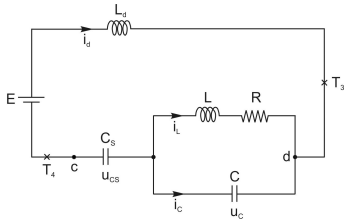


*Fig.13. Resonant circuit in the third time interval of the inverter*

The fourth operating interval $t \in \langle t_3, t_4 \rangle$ (Fig.2) begins when *T*3, *T*4 are off and continues until *T*1, *T*2 are on. The resonant circuit, switched off the supply voltage, functions like in the second interval and is illustrated in Figure 8.

## 4. CONCLUSION

The article has presented a mathematical model of electromagnetic phenomena that occur during stable operation of thyristor inverter including a series-parallel resonant circuit. Phenomena of current commutation among the circuit elements are excluded from this analytical method. Calculation results have the form of current and voltage waveforms in the circuit which are continuous at boundaries of time interval in the inverter's operation cycle. Analytical results show conformity with results of the system's simulation testing. The presented mathematical dependencies enable to analyse the system's sensitivity to variations of its parameters. However, they are highly complex.

**REFERENCES**

[1] KÁCSOR G., ŠPÁNIK P., DUDRÍK J., LUFT M., SZYCHTA E.: *Principles of operation of three-level phase shift controlled converter*, KTU Journal of Electronics and Electrical Engineering, T170 Electronics, 2008. Nr 2(82), Kaunas Lithuania, pp. 69-74 (ISSN 1392-1215)

[2] KAZIMIERCZUK M.K., CZARKOWSKI D.: *Resonant Power Converters,* A Wiley-Intersience Publication. John Wiley and Sons. Inc. New York, Toronto, Singapore 1995

[3] RODA M.R., REVANKAR G.N.: *Voltage-Fed Dis-continuous Current Mode High–Frequency Inverter for Induction Heating*, IEEE Transactions on Industrial Electronics and Control Instrumentation, vol. IECI-25 1978

[4] SZYCHTA E.: *Thyristor inverter with series-parallel resonant circuit*', Archives of Electrical Engineering, VOL.LIV No. 211, 1/2005, pp. 21–50

[5] LUFT, M., SZYCHTA, E.: *Математическая мо-дель мультирезонансного инвертора ZVS DC/DC, повышающего напряжение*, Вестник МИИТ-а, № 17, сс.74-86, Москва 2007, Россия